OBSERVATIONS WITH THE UNIVERSITY OF WISCONSIN ARCTIC HIGH SPECTRAL RESOLUTION LIDAR

Edwin W. Eloranta, Igor A. Razenkov, Joesph P. Garcia, and James Hedrick
University of Wisconsin, 1225 W. Dayton St., Madison, WI, USA,
E-mail:eloranta@lidar.ssec.wisc.edu

ABSTRACT

The University of Wisconsin Arctic High Spectral Resolution Lidar is designed for long-term untended operation in the Arctic. It has acquired more than 1-year of nearly continuous data as part of an extended shakedown test. In addition, remote operation has been demonstrated during a 2-month deployment at the ARM site in Barrow, Alaska. Examples of this data are presented to illustrate HSRL measurement capabilities.

1. INTRODUCTION

Climate models suggest that the Arctic climate is particularly sensitive to perturbation by increasing levels of greenhouse gases. This sensitivity seems to be verified by measurements which show that the Arctic is warming faster than any other part of the globe [1]. However, comparison of many climate models show wide variations in predictions for future warming. Studies of these differences show that the greatest source of uncertainty relates to the modeling of clouds. The models use different parameterizations to describe clouds resulting in very different cloud predictions. Unfortunately, very little observational data is available for verification. Arctic cloud observations have been limited by several factors including: 1) the lack of observers, 2) the difficulty of seeing clouds during the long Arctic night, 3) a lack of visual and temperature contrast between clouds and the snow surface, which impedes satellite cloud retrievals, and 4) the inconsistent reporting of diamond dust precipitation.

The University of Wisconsin has constructed a High Spectral Resolution Lidar (HSRL) for long-term Arctic cloud studies. This system, which is designed to operate as a minimally-tended Internet appliance, provides absolutely calibrated profiles of backscatter cross section, optical depth and depolarization[2][3] [4]. The ability to correct signals for attenuation without a priori assumptions makes it possible to derive reliable optical depth and backscatter cross section profiles using fully automated data processing. The lidar requires only electrical power, an Internet connection, and a zenith facing window for operation. All control and data transfer is accomplished via the Internet. No routine on site attention is required other than cleaning of the window. Use of a 4 kHz repetition rate laser and expansion of the transmitted beam through a 40 cm telescope reduces the transmitted energy density to eye-safe levels, making it possible to look directly into the output beam without hazard. A 45μrad. angular field-of-view coupled with a 8 GHz bandwidth etalon filter reduces background noise to very low levels. A high-dynamic range photon counting data system provides profiles with 7.5 m range resolution up to a maximum altitude of 30 km. Detector gain changes are not required in response to changing weather; conditions ranging from the clear atmosphere to dense low-altitude water clouds can be accommodated. In addition, the system calibration is not sensitive to changes in window transmission making it possible to derive accurate measurements during precipitation events which deposit snow and water on the output window. This paper describes measurements derived with the new HSRL during shakedown testing in our Madison, WI laboratory and while deployed in Barrow, Alaska as part of the MPACE experiment.

The lidar operates 24-hours/day and more than a year of data has been acquired in Madison with an additional 2-months of data collected in Barrow. Data is automatically transfered in real time from the lidar to our archive computer via a fault-tolerant client-server application where it is stored as netcdf files on a 1-terabyte raid disk system. All data can be accessed through a publicly accessible web site: 'lidar.ssec.wisc.edu'. Real time access is provided by a web tool which computes images and profiles on demand using: 1) the raw data, 2) weather service Radiosonde temperature profiles, and 3) system calibration data. The time and altitude interval for the data can be specified. Data may also be searched via web pages which provide a complete month of 12-hour thumbnail images of the backscatter cross section between the surface and 15 km. Clicking on an image provides a full screen version of the backscatter cross section and the depolarization

image. An online system log book provides information about system maintenance and software modifications. A web tool is provided to display system housekeeping data and a web interface is provided to process data on demand providing an output file which can be downloaded in netcdf format.

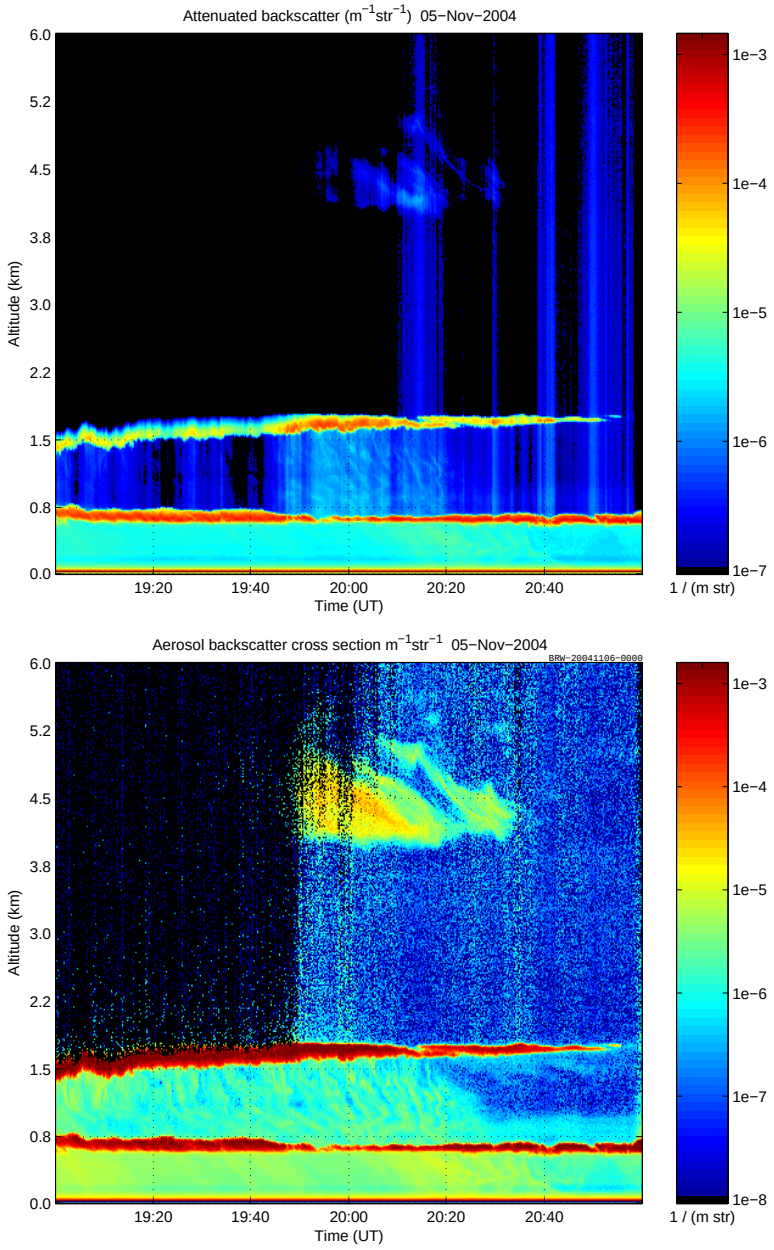

Figure 1. The r-squared, energy, and overlap corrected lidar signal measured in the combined channel(upper panel) and the HSRL derived backscatter cross section (lower panel). Data was acquired between 19:00 and 21:00 UTC on 05 Nov 2004 at the ARM site in Barrow, Alaska. The upper image, is identical to that which would be measured using a well calibrated conventional lidar; notice that low clouds shadow higher clouds. The HSRL derived image shown below is corrected for attenuation. Measurements are unaffected by attenuation until the signals are total extinguished.

Figure 1 shows images acquired on November 5, 2004 between 19:00 and 21:00 UTC. These images compare a standard lidar image of the attenuated backscatter cross section with a backscatter cross section image derived for the same period. In the conventional image (upper panel), shadows appear in the image and the attenuated backscatter cross section values depend on the presence or absence of underlying water clouds. The HSRL measured backscatter cross

section (lower panel) eliminates this dependence. Although attenuation in the lower cloud reduces the maximum altitude which can be observed, the attenuation does not affect the backscatter values where signal is present. Because the HSRL scattering cross section measurements are computed from the relative intensity of the molecular backscatter and particulate backscatter at each altitude, the values are independent of attenuation at lower levels. This provides another advantage; calibration is insensitive to dirt, water or snow on the output window.

Figure 2 presents the circular depolarization measured with the data shown in figure 1. Water clouds create little depolarization and are easily identified the blue layers in this figure while ice crystals in the cirrus layer above 3.5 km and in the snow falling from the water clouds provide depolarizations of $\sim 80\%$ and appear red in this depiction.

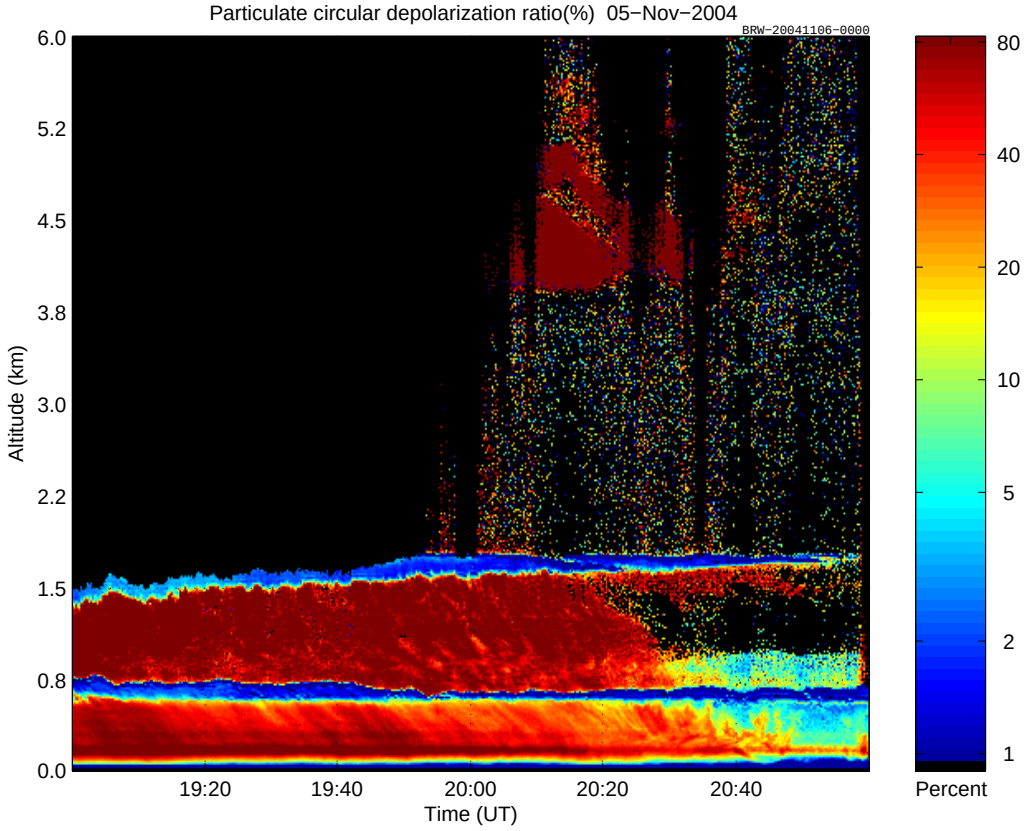

Figure 2. Circular depolarization measured between 19:00 and 20:00 UTC on 11 November 2004. Very low depolarization (blue) distinguishes water clouds from ice (red). Notice that the depolarization scale is logarithmic.

Figure 3 shows backscatter cross section and optical depth profiles created from a 3-minute average of data acquired between 20:00 and 20:03 UTC. The Rayleigh backscatter cross section computed from a Radiosonde temperature profile is shown along with the derived particulate scattering cross section and the measured attenuated-molecular scattering cross section.

Low-attitude observations are particularly important in the Arctic. Persistent stratus layers with cloud bases between 500 and 800 m were observed in in Barrow with occasional bases below 200. Snow showers often fill the volume below the stratus layer. This lidar provides useful data exceptionally close to the ground; detectors quickly recover from an initial transient and the molecular channel data is valid above 75 m and the combined channel data is valid above 200m. This illustrates effective isolation of the detectors from scattered laser light. Detector overload is often a problem in lidars which use the same telescope to receive and transmit. The molecular channel detector is exposed to approximately 10 photons, which have been scattered from optics as the laser pulse exits the system. The combined-channel photomultiplier, which is not protected by the iodine absorption filter, is exposed to approximately 200,000 photons, which, after taking into account the 5% quantum efficiency of the photomultiplier, produce approximately 10,000 photoelectons.

The backscatter cross section measurement is computed from the ratio of the molecular and combined channel signals

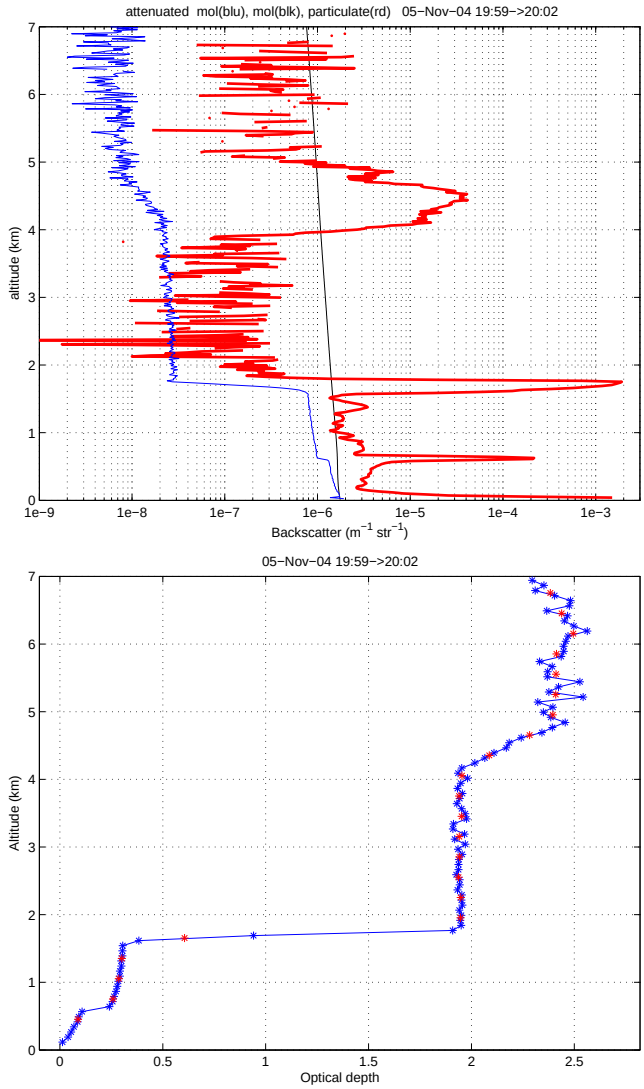

Figure 3. The aerosol backscatter cross section (top panel-red), the attenuated molecular cross section (top panel-blue), the Rayleigh backscatter cross section computed from a Radiosonde temperature profile (top panel-black) and the optical depth profile (bottom panel). Profiles are an average of data measured between 20:00 and 20:03 UTC on 5-Nov-04.

so that it is independent of any range-dependent geometric corrections. However, this is not true for the attenuated-molecular cross section profile. The angular field-of-view of the lidar is only 45μrad and the raw HSRL signals depart strongly from the standard r^{-2} dependence at altitudes below 5 km. This effect is measured as part of the system calibration and removed during data processing. These geometric corrections have proven to be very stable, reflecting the advantage of using a common telescope to transmit and receive.

The lower panel of Figure 3 shows the optical depth measured as a function of altitude above a reference point at 75 meters. This is computed from the ratio of the computed molecular cross section and the observed attenuated molecular cross section shown in figure 2. Notice the correspondence between attenuation of the molecular return shown in figure 2 and the optical depth curve. The attenuation caused by the .7 km and 1.5 km water cloud along with the 4 to 5 km cirrus clouds are directly reflected in the optical depth curve. In this case the total optical depth of the atmosphere is approximately 2.4. For short averaging times, the maximum optical depth which can be measured with the lidar is determined by photon statistics; the penetration depth increases with averaging time. For long averaging times, the maximum optical depth is currently limited to values less than 4 by detector after-pulse contributions to the molecular signal.

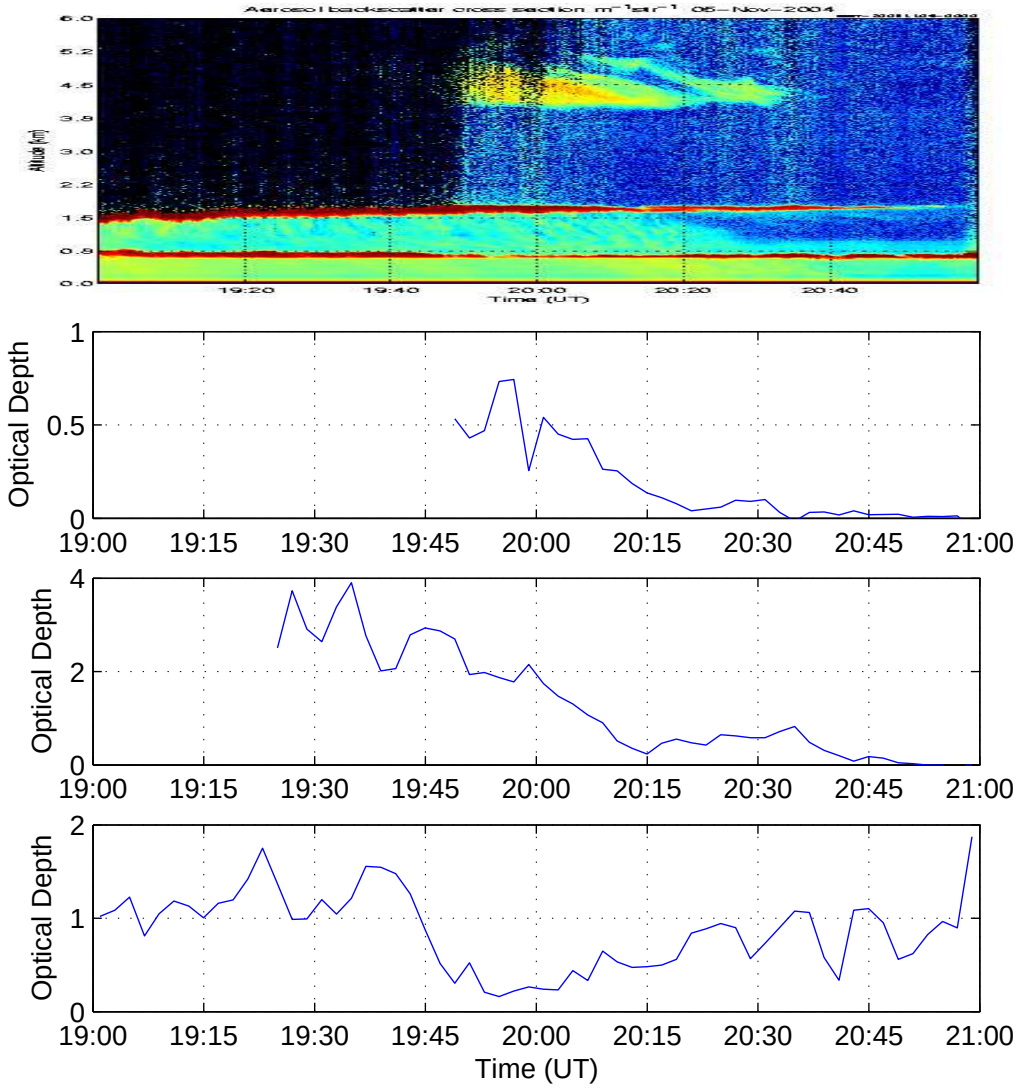

Figure 4. Optical depth as a function of time for the three separate cloud layers observed between between 19:00 and 21:00 UTC on 5-Nov-04. Optical depth between the surface and 1.3 km is shown in the bottom panel, between 1.3 and 1.9 in the middle, and between 1.9 and 6.1 in the upper panel. The backscatter cross section image is shown above the line plots for comparison.

Figure 4 shows shows the optical depths measured for three separate cloud layers as a function of time. A one-minute averaging interval was used in this case. Prior to 19:24 UT the combined optical depth of the lowest and the middle layer exceeded the measurement capability of the lidar. This also occurred for the cirrus layer prior to 19:50 UT.

Acknowledgments

This research was supported by National Science Foundation Grant OPP-9910304,

References

[1] Hassol, S. J. Impacts of a Warming Arctic. *Arctic Climate Impact Assessment, Cambridge University press, 2004*

[2] Razenkov, I. A., E. W. Eloranta, J. P. Hedrick, R. E. Holz, R. E. Kuehn, and J. P. Garcia. A High Spectral Resolution Lidar Designed for Unattended Operation in the Arctic. *Proc. ILRC21, 57-60, 2002*

[3] Pirronen, P. A high spectral resolution lidar based on an iodine absorption filter Ph.D. thesis, Univ. of Joensuu, Joensuu, Finland, pp 113, 1994.

[4] Grund, C. J. and E. W. Eloranta The University of Wisconsin High Spectral Resolution Lidar *Optical Engineering*, 30: 6-12, 1991.